Tectonophysics 602 (2013) 78–86

Contents lists available at SciVerse ScienceDirect

Tectonophysics

journal homepage: www.elsevier.com/locate/tecto

Global model for the lithospheric strength and effective elastic thickness

Magdala Tesauro [a,*], Mikhail K. Kaban [a], Sierd A.P.L. Cloetingh [b]

[a] German Research Center for Geosciences (GFZ), Potsdam, Germany
[b] Department of Earth Sciences, Utrecht University, Netherlands

ARTICLE INFO

Article history:
Received 6 March 2012
Received in revised form 19 November 2012
Accepted 10 January 2013
Available online 17 January 2013

Keywords:
Rheology
Lithosphere
Strength
Effective elastic thickness

ABSTRACT

Global distribution of the strength and effective elastic thickness (T_e) of the lithosphere are estimated using physical parameters from recent crustal and lithospheric models. For the T_e estimation we apply a new approach, which provides a possibility to take into account variations of Young modulus (E) within the lithosphere. In view of the large uncertainties affecting strength estimates, we evaluate global strength and T_e distributions for possible end-member 'hard' (HRM) and a 'soft' (SRM) rheology models of the continental crust. Temperature within the lithosphere has been estimated using a recent tomography model of Ritsema et al. (2011), which has much higher horizontal resolution than previous global models. Most of the strength is localized in the crust for the HRM and in the mantle for the SRM. These results contribute to the long debates on applicability of the "crème brulée" or "jelly-sandwich" model for the lithosphere structure. Changing from the SRM to HRM turns most of the continental areas from the totally decoupled mode to the fully coupled mode of the lithospheric layers. However, in the areas characterized by a high thermal regime and thick crust, the layers remain decoupled even for the HRM. At the same time, for the inner part of the cratons the lithospheric layers are coupled in both models. Therefore, rheological variations lead to large changes in the integrated strength and T_e distribution in the regions characterized by intermediate thermal conditions. In these areas temperature uncertainties have a greater effect, since this parameter principally determines rheological behavior. Comparison of the T_e estimates for both models with those determined from the flexural loading and spectral analysis shows that the 'hard' rheology is likely applicable for cratonic areas, whereas the 'soft' rheology is more representative for young orogens.

1. Introduction

The strength of the Earth's lithosphere, or the maximum stress it can support before deforming, has been debated since the beginning of the last century (Barrell, 1914). The present state and behavior of the Earth system depend significantly on the processes that deform the lithosphere including rifting, mountain building, sedimentary basin development, seismicity and volcanism. Knowledge of the strength distribution on a global scale is thus crucial for understanding the mechanics of these processes (e.g., Cloetingh et al., 2005). The continental lithosphere consists of a mechanically strong upper crust, which is in general separated by a weak lower crustal layer from the strong upper part of the mantle lithosphere, which in turn overlies the weak lower mantle lithosphere. Hence the strength of continental lithosphere is controlled by the thickness and composition of the crust, the temperature of the mantle lithosphere, the presence or absence of fluids, and the strain rates (e.g., Brace and Kohlstedt, 1980). In contrast, the oceanic lithosphere consists of a thin crust overlying the mantle lithosphere, and consequently its strength depends primarily on the temperature distribution (e.g., Kusznir and Park, 1987). Uncertainties in the rheological parameters, deformation mechanisms, temperatures, and assumed tectonic conditions yield uncertainties in the strength (e.g., Tesauro et al., 2010). Although new laboratory measurements (e.g., Bürgmann and Dresen, 2008) have more control on the uncertainties in the rheological parameters, these experiments utilize simple monophase minerals having a homogeneous grain size, whose extension to real aggregate compositions remains to be demonstrated. In this paper we estimate the global integrated lithospheric strength distribution for the continental areas through the integration of the yield strength envelope (YSE), which shows the rock strength as a function of depth (Goetze and Evans, 1979). To this aim we construct a set of possible end-member strength models, using 'soft' and 'hard' rheology for the continental crust. This approach allows us to identify areas where uncertainties in other factors (e.g., temperature) might play a significant role. Another important parameter, also related to the strength, is the effective elastic thickness of the lithosphere (T_e), which characterizes its response to loading (Burov and Diament, 1995) and primarily depends on the thermal gradient, composition and flexural plate curvature (e.g., Burov and Diament, 1995).

Burov and Diament (1995) suggested a method to estimate T_e for several lithospheric layers with constant Young Modulus (E). However, the lithosphere is very heterogeneous in vertical direction, and the average E of the lithospheric mantle is almost double than that of the crust. Therefore, we derive new equations to calculate T_e from the lithospheric strength distribution, considering different E for each lithospheric layer.

* Corresponding author.
E-mail address: magdala@gfz-potsdam.de (M. Tesauro).

0040-1951/$ – see front matter © 2013 Elsevier B.V. All rights reserved.
http://dx.doi.org/10.1016/j.tecto.2013.01.006

T_e is determined for the two rheological models and compared with the estimates obtained in flexural loading and spectral studies (e.g., Audet and Bürgmann, 2011; Tesauro et al., 2012a).

2. Method

The estimates of lithospheric strength and elastic thickness are based on the global distributions of crustal and mantle parameters, which are derived from existing models. The global Moho depth map (Fig. 1a) combines recent compilations for North America, Eurasia and Australia (e.g., Mooney and Kaban, 2010; Tesauro et al., 2008). In other regions we use the CRUST2.0 model (Bassin et al., 2000). Other parameters of the crust have also been revised using these new datasets. For example, the global map of the sedimentary thickness includes new compilations for the continents (Mooney and Kaban, 2010; Tesauro et al., 2008) and for the oceans (Divins, 2003).

2.1. Thermal model

We construct a 3D temperature model of the mantle by the conversion of the S-wave velocity model S40RTS (Ritsema et al., 2011) using a mineral physics approach (Cammarano et al., 2003). The new tomography model is based on a data set of about an order of magnitude larger than used in their previous one S20RTS (Ritsema et al., 2004), which was employed in the study of Tesauro et al. (2012b). The horizontal resolution of the recent model is at least two times better than the previous one, which greatly improves the final result. Following the mineral physics approach described in Cammarano et al. (2003), the anharmonic effect was calculated at a given pressure and temperature (P, T) conditions by extrapolating density and the anharmonic moduli, first in temperature and then, along an adiabat, in pressure. Voigt–Reuss–Hill (VRH) averaging (Hill, 1963) yields ρ, K_S and G at P, T for a composite mineralogy.

Uncertainty of the relative variations of seismic velocities at some depth might reach 20%. Between 100 and 150 km, the anomalies of the tomography model of Ritsema et al. (2011) span a range of $\pm 6\%$. Therefore, the maximum uncertainty of the S-wave velocity is about ~0.05 km/s, which translates into temperature changes up to ~150 °C in the cold cratons. However, we should consider that the maximum uncertainties of seismic velocity anomalies affect only the areas characterized by poor data coverage (e.g. Greenland and Antarctica). In other low-temperature zones the uncertainty is likely reduced to the half of the maximum value, causing temperature changes up to ~70 °C. The effect is notably smaller in the hot areas, where velocity variations correspond to smaller temperature changes due to anelasticity. On the other hand, assuming that the seismic model is well resolved and the composition is known, the uncertainty in temperatures may reach ± 100 °C (Cammarano et al., 2003). However, for estimation of the spatial strength variation, only temperature variations at any specific depth are important. These latter are much better constrained than the absolute temperatures. The main uncertainty of our thermal model stems from the global tomography model, which is unlikely to be well-resolved at scales of less than ~500 km in many locations not seismically well-sampled at those scale. Other uncertainties depend on temperature derivatives of the elastic parameters, which are estimated to be between 10% and 20% (e.g. Cammarano et al., 2003), leading to uncertainty in the inferred temperatures of about ± 70 °C above 300 km (Tesauro et al., 2010). Other factors (e.g. composition, water and partial melt) also affect seismic velocities, resulting in uncertainties in the temperature determinations. The maximum temperature uncertainty due to composition is ~150 °C at shallow depths (<120 km). At greater depths, this uncertainty is reduced to about

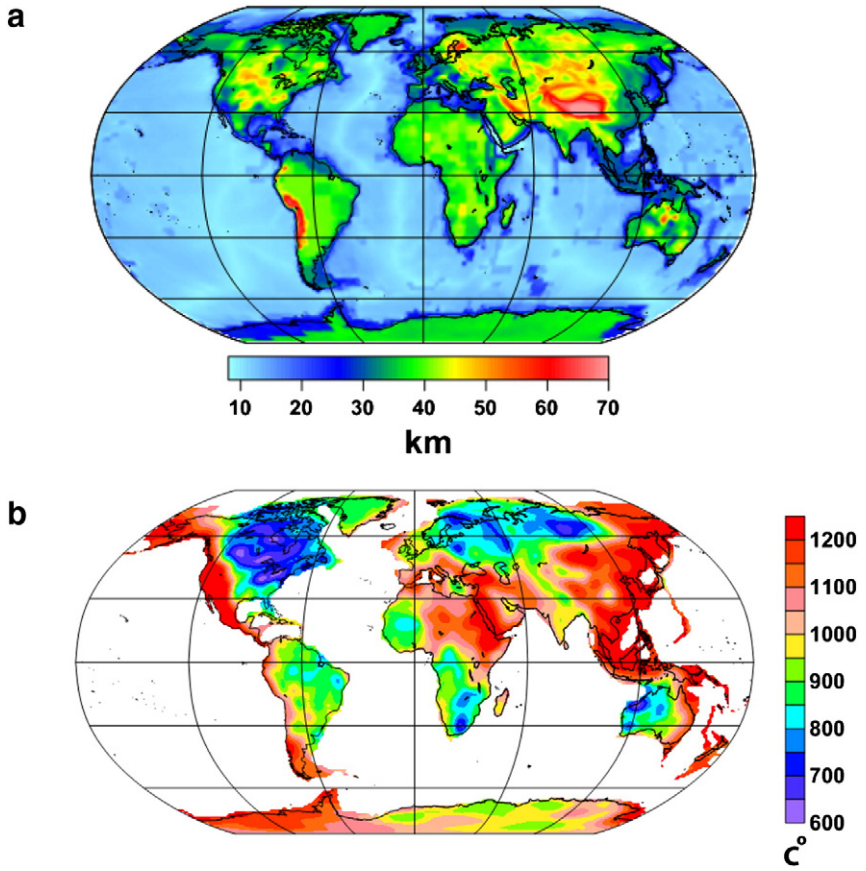

Fig. 1. (a–b) Examples of the input parameters for the strength and Te models. (a) Moho depth (km); (b) Temperature at 100 km depth.

65 °C, on account of the anelasticity effect (e.g. Hyndman et al., 2009). Therefore, the compositional effect is particularly important for the cold Achaean cratons (Hieronymus and Goes, 2010). In contrast, in the tectonically active areas, the melting temperature is reached at shallow depths (about 100 km) and the effect of the compositional differences is strongly reduced. For those areas, the main uncertainty is due to the anelasticity model used (Shapiro and Ritzwoller, 2004). To reduce the uncertainties related to compositional variations, we use the compositions which are representative for the mantle lithosphere over large areas, such as 'Proton-Archon' in the cratons (Griffin et al., 2003), which is depleted in the iron content, and 'PrimitiveMantle' (McDonough and Sun, 1995) outside the craton. The 'Proton-Archon' composition might underestimate the effect of the stronger iron depletion typical for some Archean cratons, which translates in the underestimation of the temperature by 100–150 °C. We chose the anelasticity model (Q_5) that gives intermediate estimates between the other two (Q_4 and Q_6) (Cammarano et al., 2003). On the other hand, the drier conditions in the cratons lead to the overestimation of the temperature up to ~200 °C. The effect of water and melt content on seismic velocities is important for high-temperature zones like the oceanic areas. However, seismological data (Forsyth et al., 1998) show that at the mid-ocean ridges the partially molten area corresponds to a narrow band (<100 km) of the lithosphere younger than a few My. Therefore, the uncertainties of the tomography model, likely affect the temperatures more strongly and correspondingly influence the strength and elastic thickness models. In general, the mantle geotherms predicted by our thermal model agree well with those obtained in previous studies based on the observed heat flow (Artemieva and Mooney, 2001). However, lateral variations in temperature are better imaged in our model, on account of the high resolution of the input tomography data.

The temperature at depth of 100 km is characterized by strong lateral variability (Fig. 1b), even between 600 °C and 950 °C in the Achaean and Proterozoic cratons. Temperatures in the younger continental areas are already close to the melting point (1200 °C–1300 °C). The mantle density was estimated as a function of pressure and temperature (e.g. Cammarano et al., 2003). Temperatures were extrapolated to the surface using typical crustal isotherms determined for different tectonic provinces on the base of the characteristic values of the radiogenic heat production for each crustal layer (e.g. Čermák, 1993). Mechanical properties of the mantle may change gradually in the vicinity of the solidus. Consequently, no sharp boundary between the mechanically weak lithosphere and the asthenosphere (LAB) possibly exists (Cammarano et al., 2003). Therefore, the LAB was defined as the 1200 °C isotherm, intermediate between the 1300 °C (mantle solidus temperature) and 1100 °C (0.85 of the mantle solidus temperature) isotherm (Artemieva and Mooney, 2001).

2.2. Integrated strength

The yield strength envelope (YSE) is represented by the curves of two different types (Fig. 2). At shallow depths the straight line corresponding to brittle fracture shows the increase of the strength with depth. At deeper levels, the curved line that describes ductile deformation shows that strength decreases downward exponentially due to the increase of temperature and corresponding decrease of viscosity (Burov and Diament, 1995). The depth at which the brittle and ductile strengths are equal is defined as the brittle–ductile transition (BDT). The integrated lithospheric strength (σ_L) is estimated through the integration of the YSE (Eq. (1)),

$$\sigma_L = \int_0^h (\sigma_1 - \sigma_3)\cdot dz \tag{1}$$

where h is the thickness of the lithosphere and σ_1 and σ_3 the maximum and minimum principal components of the stress tensor.

The strength for the brittle regime, as described by Byerlee's law (Byerlee, 1978), is a function of pressure and depth independent of rock type. As a result, the total strength of a brittle layer is:

$$\sigma = f\rho g z(1-\lambda) \tag{2}$$

where f is the friction coefficient, ρ the density, g the acceleration of gravity, z the depth of the bottom of the layer, and λ is the pore fluid factor. The friction coefficient is equal to 0.75 and 3, for extensional and compressional conditions, respectively (e.g., Afonso and Ranalli, 2004). The pore fluid factor is 0.36, which is a typical hydrostatic value. In a recent study of Pauselli et al. (2010) the strength is estimated including, in addition to frictional sliding, a high-pressure brittle fracture mechanism. The introduction of the latter, usually neglected in the estimation of rheological profiles, is subject to the uncertainties of its own, but has the effect of "cutting off" brittle peaks in strength (>1 GPa) which might be unrealistic. Since this brittle mechanism is derived from experiments on only a few rock types and reduces only the peak strength, but has little effect on lateral variations, we do not consider this effect.

The ductile strength depends non-linearly on the strain rate (and thus on the time scale of the deformation process), on rock type and temperature, and also on grain size (macro and microstructure). In particular, it is extremely sensitive to temperature and presence of fluids. A slight variation in the background geotherm of the continental crust can turn its behavior predicted by strongest dry flow laws into those predicted by weakest wet flow laws. Furthermore, the geotherm also affects the brittle strength of the lithosphere through the influence of temperature on the depth of the BDT (e.g., Burov, 2011). Various mechanisms of ductile deformation exist, including diffusion creep and various mechanisms of dislocation creep. The first mechanism is predominant for small grain size and relatively low stresses, which arise for highly sheared material (ductile shear zones) or for very high temperatures. Therefore, it is of secondary importance for most pressure and temperature conditions (e.g., Burov, 2011) and is not incorporated in our model. In contrast, at high stresses and moderate temperatures (<1330 °C), the creep rate is dominated by dislocation creep, power law (Eq. (3)) and Dorn law (Eq. (4)) for crustal and mantle stresses.

$$\sigma = \left[\frac{\dot{\varepsilon}}{A_P}\right]^{\frac{1}{n}} \cdot \exp\left[\frac{E_P}{nRT}\right] \tag{3}$$

$$\sigma = \sigma_D\left(1 - \left[-\frac{RT}{E_D}\cdot \ln\left(\frac{\dot{\varepsilon}}{A_D}\right)\right]^{1/2}\right). \tag{4}$$

Here $\dot{\varepsilon}$ is the strain rate, A_P the pre-exponential constant, n the power law exponent, E_P the power law activation energy, R, the gas constant, T the temperature, σ_D the Dorn law stress, E_D, the Dorn law activation energy, A_D Dorn law strain rates. Recent experimental results on olivine in anhydrous conditions demonstrate different Dorn law behavior (Mei et al., 2010). However, in the end the depth-averaged strength, estimated with the new law, is very similar to that one obtained (Eq. 4) from the previous results of Goetze and Evans (1979).

In the 'soft rheology model' (SRM) we assign the 'dry quartzite' and 'wet diorite' rheologies to the upper and lower crust, while in the 'hard rheological model' (HRM) we assign the 'dry granite' and 'mafic granulite' rheologies. These rheologies are taken as possible end-members for the continental crust. Indeed, the high values of *Vp* and *Vs* in the old cratons likely correspond to granites and mafic granulites. On the other hand, the areas of recent deformations (e.g. the Alpine-Himalayan fold belt) are usually characterized by low values of *Vp* and *Vs*, which are typical for the quartzite–diorite composition.

We do not specify any rheology for sediments, because they are normally affected only by brittle deformation. For the mantle lithosphere we use 'dry olivine' rheology. In doing so, we suppose that a

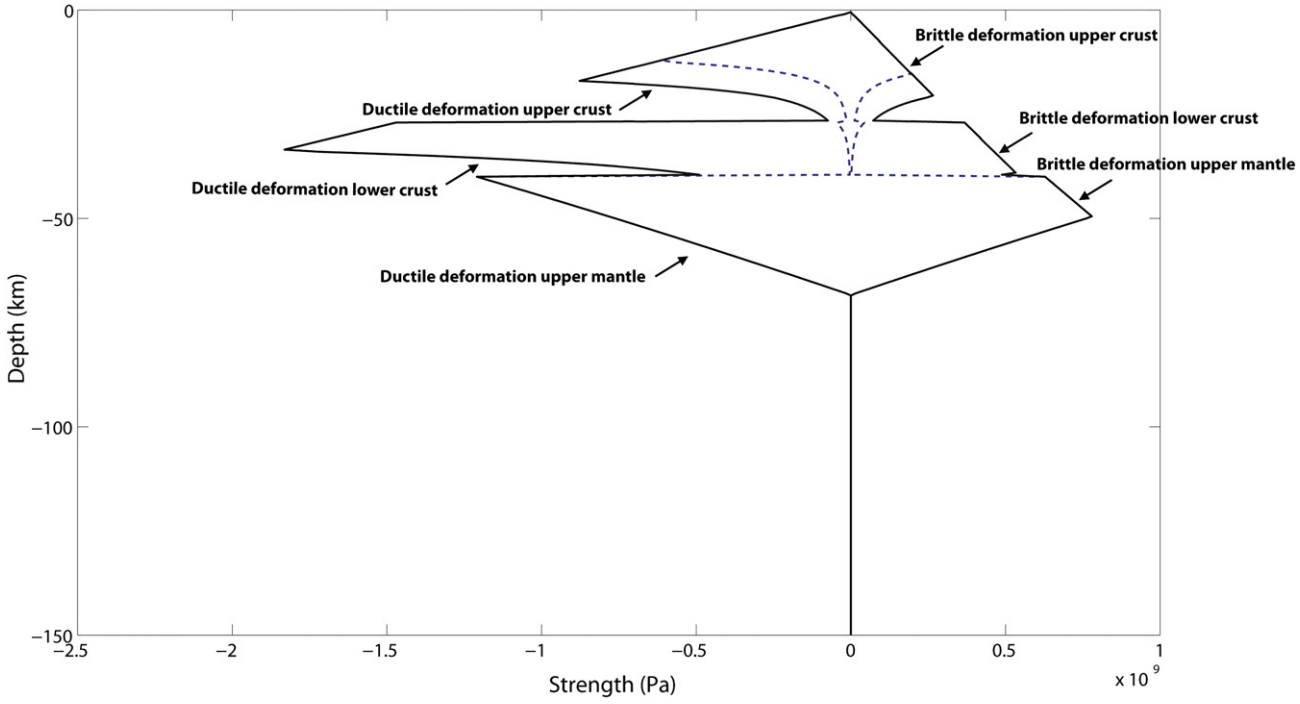

Fig. 2. Example of a yield strength envelope (YSE). The Strength is estimated for the 'soft' rheological model (SRM) (dashed lines) and the 'hard' rheological model (HRM) (black lines). For convention values estimated under compressional and extensional conditions are assumed negative and positive, respectively.

'wet' mantle model might be more suitable for areas recently affected by subduction of the oceanic lithosphere and/or by tectonothermal events (e.g., Afonso and Ranalli, 2004). Therefore, the strength values can be considered as upper bounds of those possible for the estimated thermal and crustal rheological conditions. For simplicity, some parameters were taken as uniform (e.g., strain rate, pore fluid factor, mantle rheology), representing the 'average conditions', which likely approach the 'real conditions' of the study area.

It should be noted that the strain rate may vary from ~10^{-13} s^{-1} (for the areas that deform fast) to 10^{-17} s^{-1} (for the stable areas), causing a difference in the ductile strength up to ~50%. The strain rate is uncertain. Since the primary goal of this study is to estimate the effect of the alternative crustal rheologies, we use the average constant value, which allows not to introduce further uncertainty due to a not always well-constrained parameter. In this way, we estimate the maximum possible lateral variation of the strength and T_e, depending on different crustal rheologies. Indeed, a larger strain rate in the active tectonic areas and a lower strain rate in the stable areas (e.g., the cratons) would reduce the lateral variation in strength and T_e observed in these regions. At the same time, an increase of the pore fluid factor (to simulate the presence of larger hydrostatic pressure) to values of 0.6 and 0.8 might decrease the integrated strength by 25% and 50%, respectively (Tesauro et al., 2010). The values of the rheological parameters are given in Table 1. As discussed in the previous section, possible uncertainties related to the thermal model may affect the strength estimations. However, their contribution

Table 1
Rheological model parameters and strength equations. Numbers in square brackets stand for the original source as it follows: [1] Carter and Tsenn (1987); [2] Wilks, and Carter (1990); [3] Goetze and Evans (1979).

Parameter	Symbol	Units	Sediments	Upper crust	Lower crust	Upper mantle
Composition	–	–	–	Quartzite (dry)[1]/granite(dry)[1]	Mafic-granulite[2]/diorite (wet) [1]	Olivine (dry) [3]
Density min–max/mean	ρ	km/m^{-3}	1700–2776/2346	2617–2862/2804	2886–3122/3037	3312–3380/3352
Layer Thickness min–max/mean	z	km	0–21.5/2	1.5–51.5/24	0.5–32/9.5	5–254/118
Friction Coefficient ext/com	f	–	0.75/3	0.75/3	0.75/3	0.75/3
Pore fluid factor	λ	–	0.36	0.36	0.36	0.36
Power law exponent	n	–	–	2.72/3.3	4.2/2.4	3
Power law activation energy	E_p	KJ mol^{-1}	–	134/186	445/212	510
Power law strain-rate	A_p	Pa $n^{-1}s^{-1}$	–	6.03×10^{-24}/3.16×10^{-26}	8.83×10^{-22}/1.26×10^{-16}	7.0×10^{-14}
Dorn law activation energy	E_D	KJ mol^{-1}	–	–	–	535
Dorn law strain-rate	A_D	s^{-1}	–	–	–	5.70×10^{11}
Dorn law stress	σ_D	Pa	–	–	–	8.5×10^{9}
Strain rate	ε	s^{-1}	–	10^{-15}	10^{-15}	10^{-15}
Brittle strength	$\sigma = f\rho g z(1-\lambda)$					
Creep equations						
Power law creep	$\sigma = \left[\frac{\dot{\varepsilon}}{A_P}\right]^{\frac{1}{n}} \cdot \exp\left[\frac{E_P}{nRT}\right]$					
Dorn law creep	$\sigma = \sigma_D\left(1-\left[-\frac{RT}{E_D}\cdot\ln\left(\frac{\dot{\varepsilon}}{A_D}\right)\right]^{1/2}\right)$					

chiefly depends on the uncertainties of the tomography model, which are difficult to estimate.

2.3. Effective elastic thickness (T_e)

We estimate T_e based directly on the estimated depth-distribution of strength. From the computed YSE it is possible to define mechanical thickness of each competent layer, which extends from the top of the layer to the depth associated to a specific geotherm (e.g., ~750 °C for olivine and ~350 °C for quartzite), at which the yield stress is less than some pre-defined value (e.g. 10 MPa used in Ranalli, 1994). Therefore, the lithospheric layers are considered decoupled when the strength decreases below this threshold, or welded otherwise. Then, according to Cloetingh and Burov (1996), when the lithosphere consists of n competent layers decoupled from each other, T_e is defined as follows (see also Burov and Diament, 1995):

$$T_e^{(n)} = \left(\sum_{i=1}^{n} \Delta h_i^3 \right)^{1/3} \tag{5}$$

where Δh_i is the thickness of the i_{th} competent layer. Alternatively, if the layers are mechanically coupled, the upper limit of T_e is estimated as total thickness of the competent layers:

$$T_e^{(n)} = \left(\sum_{i=1}^{n} \Delta h_i \right). \tag{6}$$

However, these equations are valid only in the case when all layers are characterized by the same Young Modulus (E). In previous studies T_e, as thickness of the equivalent homogeneous layer with the same flexural rigidity, is usually referred to the Young Modulus, $E =$ 100 GPa. However, the real lithospheric layers are characterized by significantly different values of E. Therefore, we modify the approach by Cloetingh and Burov (1996), and re-estimate T_e taking into account depth variations of E. Assuming that flexural rigidity of a homogeneous plate $\left(D_0 = \frac{E_0 Te_0^3}{12(1-\sigma_0^2)} \right)$ is equal to the flexural rigidity of a heterogeneous plate $\left(D_1 = \frac{E_1 Te_1^3}{12(1-\sigma_1^2)} \right)$, we obtain:

$$\left(T_{e0} = \sqrt[3]{\frac{E_1}{E_0}} T_{e1} \right), \tag{7}$$

where $E_0 = 100$ GPa is the reference value, E_1 is the Young modulus estimated as the Voigt (weighted) average of E of all coupled lithospheric layers (e.g. Altenbach, 2000). T_{e1} is the total thickness of the coupled competent layers, Eq. (6). In the case of decoupling conditions, T_{e1} is estimated according to Eq. (7) for each of the separate layers (or for two coupled layers and one separate) and then the Eq. (5) can be directly applied with the modified values.

Based on the assumed crustal rheology and on the experimental results of Christensen (1996), we assign $E = 90$ GPa for the upper crust and for the lower crust of the SRM and the HRM 100 and 110 GPa, respectively. The Young modulus of the lithospheric mantle is greater than of the crust (nearly the double). Despite it depends on composition, as well as on pressure and temperature variations, in the range of brittle conditions, these parameters have a small effect on E (<10 GPa). This uncertainty influences T_{e0} insignificantly (of about 1 km). Therefore, we can assume a constant value of E (180 GPa) for the lithospheric mantle.

3. Discussion

The integrated strength estimates using the SRM and HRM are displayed in Fig. 3(a–b). In the first model, zones of very high strength occur in the inner part of the cratons, while in the second one these areas are more widespread, including entire cratons and adjacent regions. The SRM and the HRM result in a different strength partitioning between the lithospheric mantle and the crust (Fig. 4(a–b)). The rheological variation causes also the significant changes of the thickness of the competent crustal layers. In order to investigate this effect, we have estimated a percentage of each competent layer with respect to the total thickness of the same layer for both the SRM and HRM (Fig. 5a–d). We can observe that the thickness of the mechanically strong part of the upper crust (MSUC) significantly increases (from 40% of the thickness of the upper crust for the SRM to ~70% for the HRM) only for the Meso-Cenozoic orogens, being equal to the thickness of the entire upper crustal layer in the other regions (Fig. 5a–b). On the other hand, the same rheological change causes an increase of the thickness of the mechanically strong part of the lower crustal layer (MSLC) from zero to 100% in most of the continental areas. Therefore, the change of the diorite content in the mafic garnet granulite rheology has more influence on the strength and T_e estimates than the change of quartzite in the granite rheology. The exception is the cratons, where the rheological variations have no effect on the MSLC for both models (Fig. 5c–d). Changing from the 'soft' to the 'hard' rheological model turns most of the continental areas from the totally decoupled mode to the fully coupled mode at the layers' boundaries (Fig. 6(a–b)). However, in areas characterized by a high thermal regime and crustal thickness (e.g., the Andes or Tibetan Plateau) the layers remain decoupled even for the HRM. At the same time, for the coldest part of the cratons the lithospheric layers are coupled in both rheological models.

For the SRM, the case in which the crustal layers are decoupled and the lower crust is coupled to the upper mantle, is not found, on account of the weakness of the lower crust in the regions characterized by an intermediate-high thermal regime. On the other hand, in the HRM, the case in which the crustal layers are coupled and the lower crust is decoupled from the mantle, is not detected. This implies that the lower crust is decoupled from the mantle when also the crustal layers are decoupled. This occurs only in the regions characterized by large crustal thickness and high thermal regime (e.g. The Andes and the Tibetan Plateau). Therefore, we may conclude that for the SRM, the areas with the strength mostly localized in the mantle, the 'jelly sandwich' model is more applicable, since the upper mantle is stronger than the crust and lower crust is the weakest layer.

For the HRM, all layers are strong and coupled in most continental areas, and the strength distributed in the whole lithosphere. Therefore, in these regions the HRM increases strongly the contribution of the crustal layers (and in particular of the lower crust) to the strength and T_e, but the mantle contribution remains significant. A 'crème brulee' model, in which the mantle is weak and the strength is primarily localized in the crust (in particular in the uppermost part where the earthquakes are located, Jackson, 2002), is applicable to the regions having a very thick crust and characterized by a high thermal regime for both the SRM and HRM, such as the Tibetan Plateau, central Mongolia and the Andes. For the HRM, there exist geological provinces normally characterized by average-to-high crustal thickness and/or by a high thermal regime (e.g. the Arabian shield, Basin and Range, part of the African metacraton and South-Eastern Australia), which have a weak mantle but strong crustal layers. This condition might be considered as a sort of the 'crème brulee' model, since the mantle is the weakest layer. The T_e values for the two strength models (T_{eS} and T_{eH}, respectively) change only moderately (<10 km) in areas where the coupling–decoupling conditions remain constant (Fig. 7(a–b)). In other continental regions, characterized by 'average' lithospheric temperature and crustal thickness, drastic variations (about ±40 km) in the T_e estimates

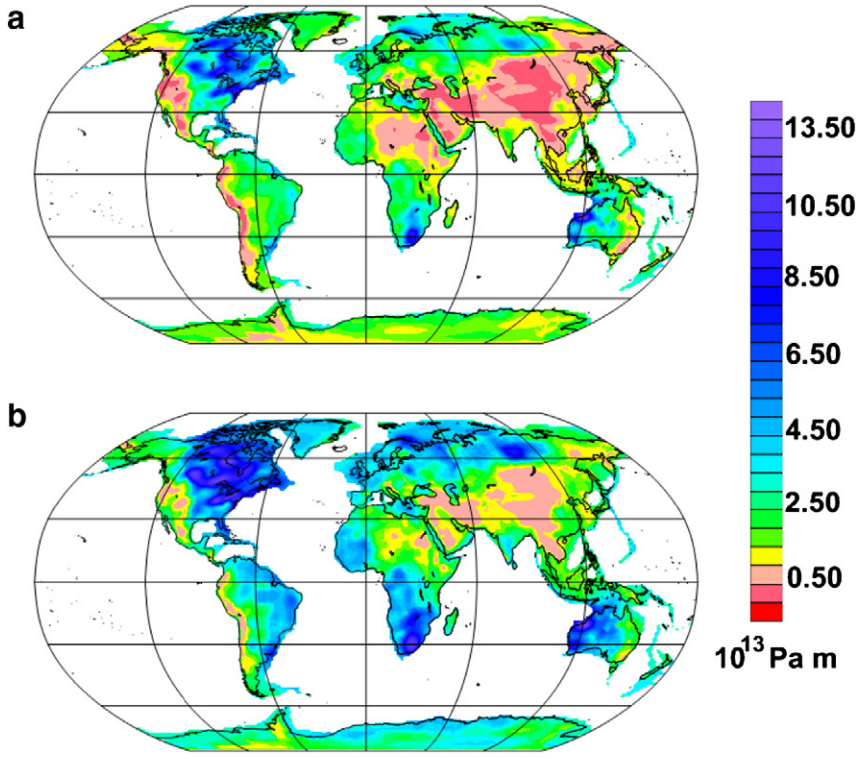

Fig. 3. (a–b) Integrated strength (Pa m) under compression for (a) 'soft' rheology model (SRM); (b) 'hard' rheology model (HRM).

are predicted. Therefore, the temperature estimates are especially crucial in these areas, because the uncertainties in rheology significantly affect the strength values.

In Table S1 we compare the ranges of T_e estimated from the SRM and the HRM models for the main continental tectonic provinces with the average T_e values (T_{eobs}) estimated from spectral and flexural loading studies (e.g., Audet and Bürgmann, 2011; Tesauro et al., 2012a). We can observe that T_{eobs} is sometimes affected by large uncertainties (>20 km). However, the lack of such error's estimation in some cases prevents us from displaying the uncertainties' range of T_{eobs}, which instead are represented as average values for each tectonic province.

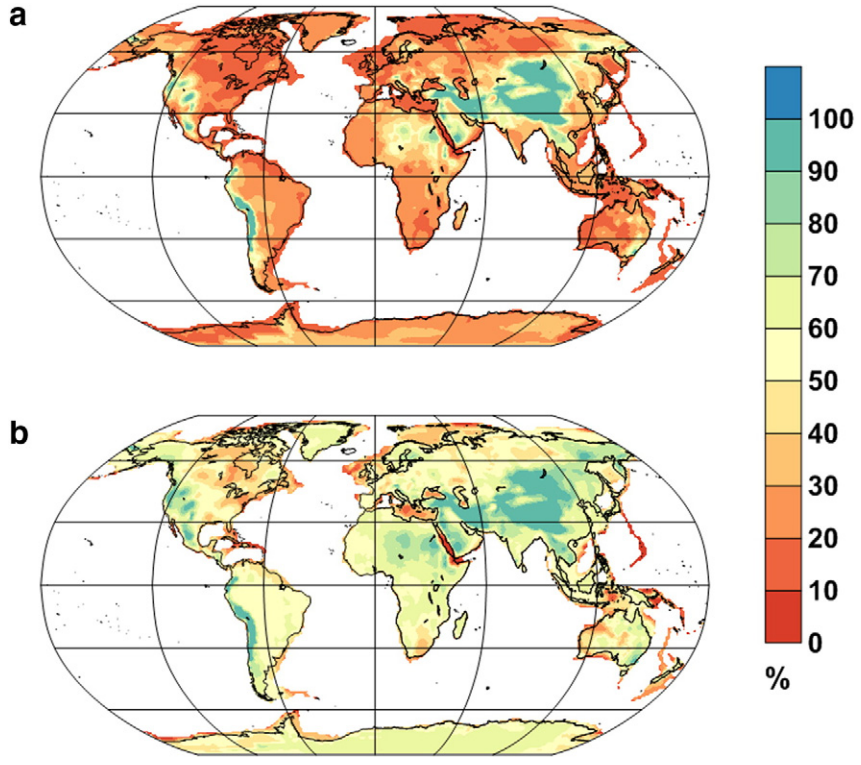

Fig. 4. (a–b) Fraction of the integrated total strength contributed by the crust for (a) SRM; (b) HRM.

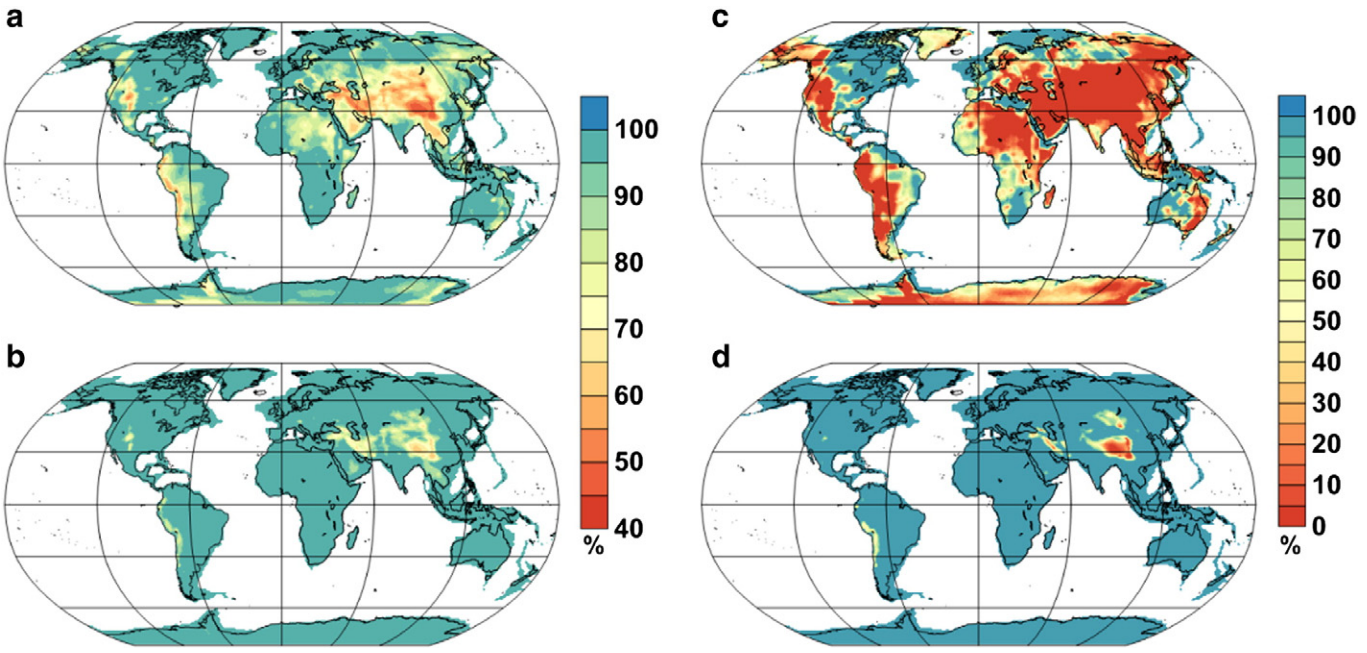

Fig. 5. (a–d) Percentage of the mechanically strong part of the crustal layers with respect to their total thickness for the 'soft' rheological model (SRM) and the 'hard' rheological model (HRM). (a) Percentage of the mechanically strong upper crustal (MSUC) thickness relative to its thickness for the SRM; (b) Percentage of the mechanically strong upper crustal (MSUC) relative to its thickness for the HRM; (c) Percentage of the mechanically strong lower crustal (MSLC) thickness relative to its thickness for the SRM; (d) Percentage of the mechanically strong lower crustal (MSLC) thickness relative to its thickness for the HRM.

The T_{eobs} estimated from flexural loading and spectral analysis is low (<30 km) in areas of active rifting and in most young orogens, which is in general agreement with the range of current estimates (Fig. 7(a–b) and Table S1). In these regions, as shown by the representative strength envelopes (Fig. 7), the crust provides the main contribution to the T_{eobs}. However, some Meso-Cenozoic orogens (e.g. Caucasus, Zagros mountains) are characterized by high values of T_{eobs} > 40 km, falling in the range of T_{eH}. The cratons and Paleozoic orogens (e.g., the Urals and the Appalachians) are characterized by high T_{eobs} (>60 km) in agreement with both rheology models (Table S1). In these regions the strength profiles include a significant contribution from the mantle lithosphere, which also affects T_{eobs}. An exception is the Siberian Craton, for which available T_{eobs} are substantially different (Table S1) with average values within the range of T_{eS}. Early Paleozoic (e.g. the Moesian Platform and Patagonia) or Proterozoic provinces (e.g. Tarim basin, Chaco basin), which are not part of the cratons and orogens, display average T_{eobs} values in agreement with both T_{eS} and T_{eH}.

4. Conclusions

We present global strength and T_e models for the end-member rheologies that define a possible range of the real lithospheric conditions. The use of the most recent crustal and lithospheric models as input parameters and of the new equations with variable Young modulus for T_e estimations increases the robustness of the results. The largest differences between the end-member models in the predicted strength and T_e distributions and in the strength partitioning between the crust and the mantle are found in areas characterized by an 'average' thermal regime and often by a limited level of seismicity and surface deformations. Thus it appears that in these areas uncertainties in temperature estimates influence the strength results significantly, since temperature is one of the principal parameters that control rheology. Comparison of the T_e values estimated from the two models with those obtained from the flexural loading and spectral analysis reveals that a 'hard' rheology is characteristic for cratonic areas, whereas a 'soft' rheology is more representative for young orogens.

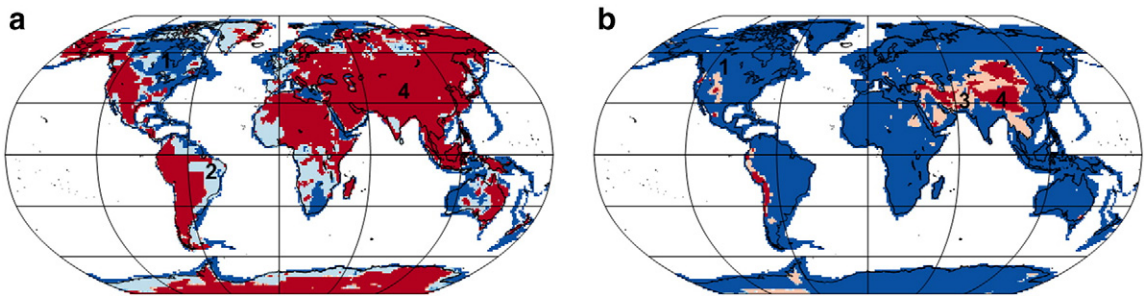

Fig. 6. (a–b) Coupling and decoupling conditions for (a) the 'soft' rheological model (SRM); (b) the HRM. Numbers are as follows: 1, crustal layers and mantle lithosphere coupled (in blue); 2, crustal layers coupled and mantle lithosphere decoupled (in azure); 3, crustal layer decoupled and mantle lithosphere coupled (in pink); 4, crustal layers and mantle lithosphere decoupled (in red).

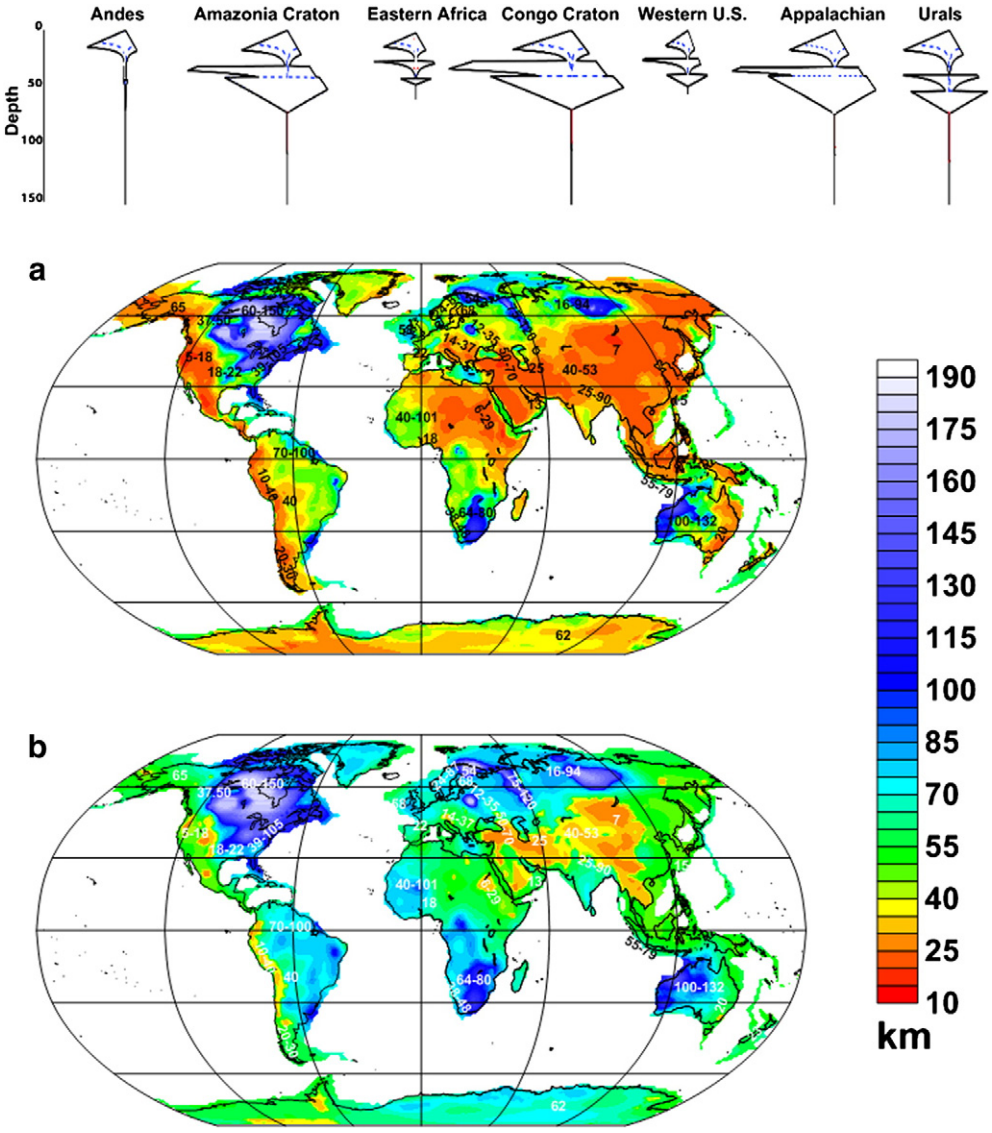

Fig. 7. (a–b) Effective elastic thickness (T_e) of the lithosphere (km) estimated from the strength distribution obtained using (a) 'Soft' rheological model (SRM); (b) 'Hard' rheological model (HRM). Numbers show the range of T_e derived from spectral and flexural loading studies for different geological provinces. Strength profiles estimated for the SRM (dashed blue lines) and for the HRM (black lines) are displayed for comparison.

Acknowledgments

We would like to thank the Editor Sean Willet, Sergei Medvedev and an anonymous reviewer for constructive reviews of this paper. We are grateful to Evguenii Burov for his suggestions. This study was funded by the Alexander von Humboldt Foundation post-doctoral grant, DFG (German Research Foundation) RO-2330/4-II and the Netherlands Research Centre for Integrated Solid Earth (ISES)

Appendix A. Supplementary data

Supplementary data to this article can be found online at http://dx.doi.org/10.1016/j.tecto.2013.01.006.

References

Afonso, J.C., Ranalli, G., 2004. Crustal and mantle strengths in continental lithosphere: is the jelly sandwich model obsolete? Tectonophysics 394, 221–232.
Altenbach, H., 2000. An alternative determination of transverse shear stiffnesses for sandwich and laminated plates. International Journal of Solids and Structures 37, 3503–3520.
Artemieva, I.M., Mooney, W.D., 2001. Thermal thickness and evolution of Precambrian lithosphere: a global study. Journal of Geophysical Research 106B, 16387–16414.
Audet, P., Bürgmann, R., 2011. Dominant role of tectonic inheritance in supercontinent cycles. Nat. Geosci. 4, 184–187. http://dx.doi.org/10.1038/ngeo1080.
Barrell, J., 1914. The strength of the Earth's crust. Part I: geologic tests of the limits of the strength. Journal of Geology 22, 28–48.
Bassin, C., Laske, G., Masters, G., 2000. The current limits of resolution for surface wave tomography in North America. Eos Trans American Geophysical Union 81 (48) (Fall Meet. Suppl., Abstract F897).
Brace, W.F., Kohlstedt, D.L., 1980. Limits on lithospheric stress imposed by laboratory experiments. Journal of Geophysical Research 85, 6248–6252.
Bürgmann, R., Dresen, G., 2008. Rheology of the lower crust and upper mantle: evidence from rock mechanics, geodesy and field observations. Annual Review of Earth and Planetary Sciences 36, 531–561.
Burov, E.B., 2011. Rheology and strength of the lithosphere. Marine and Petroleum Geology 28, 1402–1443.
Burov, E.B., Diament, M., 1995. The effective elastic thickness (*Te*) of continental lithosphere. What does it really means? Journal of Geophysical Research 100, 3895–3904.
Byerlee, J.D., 1978. Friction of rocks. Pure and Applied Geophysics 116, 615–626.
Cammarano, F., Goes, S., Vacher, P., Giardini, D., 2003. Inferring upper-mantle temperatures from seismic velocities. Physics of the Earth and Planetary Interiors 138, 197–222.
Carter, N.L., Tsenn, M.C., 1987. Flow properties of continental lithosphere. Tectonophysics 136, 27–63.
Čermák, V., 1993. Lithospheric thermal regimes in Europe. Physics of the Earth and Planetary Interiors 79, 179–193.

Cloetingh, S., Burov, E.B., 1996. Thermomechanical structure of European continental lithosphere: constraints from rheological profiles and EET estimates. Geophysical Journal International 124, 695–723.
Cloetingh, S.A.P.L., et al., 2005. Lithospheric memory state of stress and rheology: neotectonic controls on Europe's intraplate continental topography. Quaternary Science Reviews 24, 241–304.
Divins, D.L., 2003. Total Sediment Thickness of the World's Oceans & Marginal Seas. NOAA National Geophysical Data Center, Boulder, CO.
Forsyth, D., Webb, S., Dorman, L., Shen, Y., 1998. Phase velocities of Rayleigh waves in the MELT experiment on the East Pacific Rise. Science 280, 1235–1238. http://dx.doi.org/10.1126/science.280.5367.1235.
Goetze, C., Evans, B., 1979. Stress and temperature in the bending lithosphere as constrained by experimental rock mechanics. Geophysical Journal of the Royal Astronomical Society 59, 463–478.
Griffin, W.L., O'Reilly, S.Y., Abe, N., Aulback, S., Davies, R.M., Pearson, N.J., Doyle, B.J., Kivi, K., 2003. The origin and evolution of Archean lithospheric mantle. Precambrian Research 127, 14–91.
Hieronymus, C., Goes, S., 2010. Complex cratonic seismic structure from thermal models of the lithosphere: effects of variations in deep radiogenic heating. Geophysical Journal International 180, 999–1012.
Hill, R., 1963. Elastic properties of reinforced solids: some theoretical principles. Journal of the Mechanics and Physics of Solids 11, 357–372.
Hyndman, R.D., Currie, C.A., Mazzotti, S., Frederiksen, A., 2009. Temperature control of continental lithosphere elastic thickness: effective elastic thickness Te vs upper mantle velocity Vs. Earth and Planetary Science Letters 277, 539–548.
Jackson, J., 2002. Strength of the continental lithosphere: time to abandon the jelly sandwich? GSA Today 12 (9), 4–10. http://dx.doi.org/10.1130/1052-5173.
Kusznir, N.J., Park, R.G., 1987. The extensional strength of the continental lithosphere; its dependence on geothermal gradient, and crustal composition and thickness. Geological Society, London, Special Publication 28, 35–52.
McDonough, W.F., Sun, S.S., 1995. The composition of the Earth. Chemical Geology 120, 223–253.
Mei, S., Suzuki, A.M., Kohlstedt, D.L., Dixon, N.A., Durham, W.B., 2010. Experimental constraints on the strength of the lithospheric mantle. Journal of Geophysical Research 115, B08204. http://dx.doi.org/10.1029/2009JB006873.
Mooney, W.D., Kaban, M.K., 2010. The North American upper mantle: density, composition, and evolution. Journal of Geophysical Research 115, B12424. http://dx.doi.org/10.1029/2010JB000866.
Pauselli, C., Ranalli, G., Federico, C., 2010. Rheology of the Northern Apennines: lateral variations of lithospheric strength. Tectonophysics 484, 27–35.
Ranalli, G., 1994. Nonlinear flexure and equivalent mechanical thickness of the lithosphere. Tectonophysics 240 (107–1), 14.
Ritsema, J., van Heijst, H.J., Woodhouse, J.H., 2004. Global transition zone tomography. Journal of Geophysical Research 109, B02302. http://dx.doi.org/10.1029/2003JB002610.
Ritsema, J., Deuss, A., van Heijst, H.J., Woodhouse, J.H., 2011. S40RTS: a degree-40 shear-velocity model for the mantle from new Rayleigh wave dispersion, teleseismic traveltime and normal-mode splitting function measurements. Geophysical Journal International 184, 1223–1236.
Shapiro, N.M., Ritzwoller, M.H., 2004. Thermodynamic constraints on seismic inversions. Geophysical Journal International 157, 1175–1188.
Tesauro, M., Kaban, M.K., Cloetingh, S.A.P.L., 2008. EuCRUST-07: a new reference model for the European crust. Geophysical Research Letters 35.
Tesauro, M., Kaban, M.K., Cloetingh, S.A.P.L., 2010. Thermal and rheological model of the European lithosphere. In: Cloetingh, S.A.P.L., Negendank, J.F.W. (Eds.), New Frontiers in Integrated Solid Earth Sciences. Springer-Verlag, Berlin, pp. 71–101.
Tesauro, M., Audet, P., Kaban, M.K., Bürgmann, R., Cloetingh, S.A.P.L., 2012a. The effective elastic thickness of the continental lithosphere: Comparison between rheological and inverse approaches. Geochem. Geophys. Geosys. 13 (9), Q09001. http://dx.doi.org/10.1029/2012GC004162.
Tesauro, M., Kaban, M.K., Cloetingh, S.A.P.L., 2012b. Global strength and elastic thickness of the lithosphere. Global and Planetary Change 90–91, 51–57.
Wilks, K.R., Carter, N.L., 1990. Rheology of some continental lower crustal rocks. Tectonophysics 182, 57–77.